



Hybrid membranes based on polybenzimidazoles and silica with imidazoline-functionalized surface, candidates for fuel cells applications

A.A. Lysova¹ · P.A. Yurova^{1,2} · I.A. Stenina¹ · I.I. Ponomarev³ · G. Pourcelly⁴ · Andrey B. Yaroslavtsev¹

Received: 12 August 2019 / Revised: 16 December 2019 / Accepted: 22 December 2019 / Published online: 3 January 2020
© Springer-Verlag GmbH Germany, part of Springer Nature 2020

Abstract

Hybrid membranes were prepared by incorporating silica with propyl-imidazoline groups in polybenzimidazoles (phthalide-containing PBI or PBI based on 2,6- or 2,5-pyridinedicarboxylic acids). The influence effects of the silica precursor hydrolysis conditions on the conductivity of the hybrid membranes are studied. Ionic conductivity, water uptake, phosphoric acid doping, and gas permeability of the obtained materials were found to depend on the preparation method and the silica loading. The materials with 10 wt% of functionalized silica present the highest conductivity. A decrease of hydrogen permeability is observed for low silica loadings.

Keywords Polybenzimidazole · Composite membranes · Surface-modified silica · Proton conductivity

Introduction

In the modern world, energy is an increasingly important issue. Its consumption doubles every 30 years [1]. At the same time, widely used methods of energy production lead to a significant environmental impact. This forces the development of sustainable pollution-less renewable energy sources [2–4]. There is a growing interest in solar, wind, and tidal power. However, all these sources operate intermittently [5–7]. Consequently, there is a demand for energy storage systems. In respect to long-term storage, the most promising technology is a fuel cell (FC) [8–10]. Moreover, the fuel cells are autonomous power sources. About 90% of conventional

fuel cells are the low-temperature proton-exchange membrane FCs. A fast start-up and simplicity of operation are among their main advantages. At the same time, a high humidity of the supplied gas should be maintained, as well as the high-purity hydrogen should be used [8]. This makes it impossible to use cheaper hydrogen produced by conversion of the natural gas, alcohols, or biomass [11–13]. Therefore, it is necessary to develop fuel cells able to operate at 120–200 °C and at low humidities. Under these conditions, the platinum catalytic activity is enhanced, its poisoning by carbon monoxide is diminished, and the fuel cell management is simplified [14, 15].

In this context, there is a growing interest in the membranes based on polybenzimidazoles (PBIs) doped with phosphoric acid or with inorganic hydroxides [16, 17], which are able to operate at elevated temperatures and have high chemical resistance and thermal stability. A lot of works is devoted to the development of new PBI-based polymers with different structures [18, 19], methods of their stabilization and properties improvement [20, 21], as well as their application in FCs [22, 23]. Stable performance during long-term operation up to 18,000 h at 200 mAh and temperature up to 160°C was achieved for a PBI/H₃PO₄-based hydrogen-air FC [24, 25]. However, further increase in the current density results in membrane degradation or phosphoric acid leaching [26].

Stabilization of phosphoric acid in the polymer matrix is one of the challenges in the development of PBI-membranes. The main approach is associated with incorporation of organic

✉ A.A. Lysova
ailyina@yandex.ru

✉ Andrey B. Yaroslavtsev
yaroslav@igic.ras.ru

¹ Kumakov Institute of General and Inorganic Chemistry RAS, Leninsky pr-t 31, 119991 Moscow, Russia

² National Research University Higher School of Economics, Myasnitskaya str. 20, 101000 Moscow, Russia

³ Nesmeyanov Institute of Organoelement Compounds RAS, Vavilova str. 28, 119991 Moscow, Russia

⁴ Institut Européen des Membranes, UMR 5635, Université Montpellier, ENSCM, CNRS, CC047, 34095 Montpellier Cedex 5, France

or inorganic materials with a high sorption activity [27–32]. In addition, the conductivity of PBI membranes usually correlates with the phosphoric acid content, as the latter acts both as a charge carrier and conduction medium.

Previously, we have investigated the hybrid materials based on PBI membranes with sulfonated silica [33, 34]. The incorporation of 2–5 wt% of silica nanoparticles leads to an increase in the membrane conductivity. Moreover, it was shown that the degree of conductivity increase depends on the preparation method and the microstructure of the hybrid membrane [33, 34]. At the same time, the incorporation of sulfonated silica did not promote the phosphoric acid retention, which provided the higher conductivity. Therefore, incorporation of the particles with basic surface should be more favorable [35–37].

In this regard, the aim of the present paper is to study hybrid PBI membranes containing silica particles with a surface modified by groups containing basic N-atoms. Commercially available triethoxy-3-(2-imidazolin-1-yl)propylsilane with a structure similar to PBI was used for this purpose.

Experimental

The synthesis procedures of the PBI-O-PhT polybenzimidazoles and polybenzimidazoles obtained from 2,6- or 2,5-pyridinedicarboxylic acids (PBI-2,6Py and PBI-2,5Py) are described elsewhere [34, 38]. In this study, the composite membranes were prepared by casting the solution with the pre-synthesized silica particles (the 1st method) or with a precursor for their synthesis (the 2nd method).

Preparation of the 3-(2-imidazolin-1-yl)propyl modified silica

Surface modified silica (SiO₂Im-ex) was synthesized by silanes co-condensation. A mixture of tetraethoxysilane (TEOS, Aldrich) and triethoxy-3-(2-imidazolin-1-yl)propylsilane (IPTES, Aldrich) (Fig. 1) in a molar ratio 4:1 was dissolved in isopropanol (Chimmed) and heated to 50 °C under constant stirring. Afterward, the hydrolysis by a mixture of ammonium hydroxide (1.3 mL), de-ionized water (13.6 mL), and isopropanol (35 mL) was performed. The reaction mixture was kept at 50 °C under stirring for 3 h. The obtained silica SiO₂Im-ex was washed with deionized water and dried in air.

Preparation of hybrid membranes

The hybrid membranes were obtained by casting the PBI solutions in N-methylpyrrolidone (4 g of polymer/100 mL). In the 1st method, the SiO₂Im-ex particles were prepared by

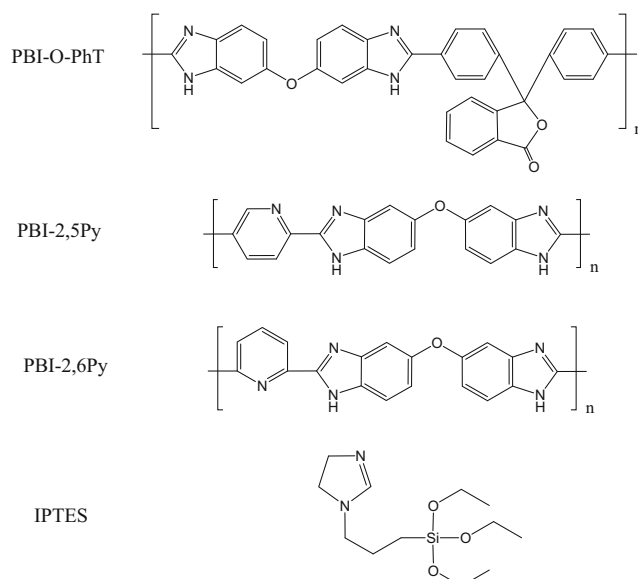


Fig. 1 Chemical structures of polybenzimidazoles and triethoxy-3-(2-imidazolin-1-yl)propylsilane

mixing PBI solution with the SiO₂Im-ex particles. In the 2nd method, a mixture of TEOS and IPTES in a molar ratio 4:1 was used as a silica precursor. The polymer solution with a fixed amount of the SiO₂Im-ex oxide or its precursor was first homogenized by ultrasonication for 5 min and then dried on a glass plate at 50–60 °C for 3 days. To remove the residual solvent, the obtained films were kept at 120 °C under vacuum. According to the 2nd method, the hydrolysis of the introduced silanes was carried out at the next step. The films with silica particles formed directly within the polymer matrix (SiO₂Im-in) were thus obtained. In both cases, the silica content varies from 0 to 20 wt%. The polymer type, the silica type, its loading is indicated in the sample name, for example, PBI-O-PhT/SiO₂Im-ex-15 or PBI-2,6Py/SiO₂Im-in-10.

To increase the conductivity, all the obtained samples were treated by phosphoric acid at 25 °C for 7 days. Its concentration was 75% and 60% for PBI-O-PhT and PBI-2,5Py (PBI-2,6-Py), respectively. After the treatment, the weight of the membranes increased by 2–3 times. Finally, the samples were dried under vacuum at 70 °C for 4 h and kept in a desiccator over P₂O₅.

Material characterization

Infrared absorption spectra were recorded using the Nicolet iS5 Fourier Transform Infrared Spectrometer in the 4000–400 cm⁻¹ range.

The phosphoric acid doping degree (the number of H₃PO₄ molecules per PBI repeat unit) was determined from the weight of the absorbed acid as reported previously [33].

The membrane morphology was studied by scanning electron microscopy (SEM) using the Carl Zeiss NVision 40

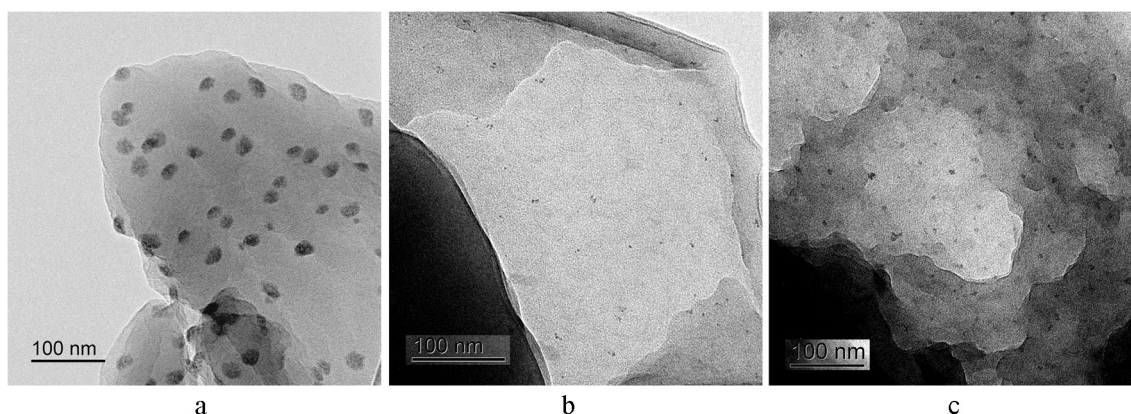


Fig. 2 TEM micrographs of the PBI-O-PhT/SiO₂-in-5 samples obtained by hydrolysis with 18% HCl solution at 25 °C (a) and 12% NH₄OH solution at 25 (b) and 50 °C (c)

scanning electron microscope equipped with Oxford X-Max EDS detector. The microstructure of the samples was studied using the Jeol JEM 2100 transmission electron microscope (TEM).

CHN-analysis was carried out using the EuroVector EA3000 elemental analyzer.

X-ray powder diffraction was carried out using the Rigaku D/MAX 2200 diffractometer, CuK_α radiation.

Specific surface of the samples was determined by capillary nitrogen adsorption (BET method) at −196 °C using the Sorbtometer-M system (“Katakron” LLC, Russia). The samples were preliminary degassed at 200 °C for 1 h.

The membrane water uptake was determined by thermogravimetric analysis (TGA) using the Netzsch TG 209 thermobalance in aluminum crucibles using a heating rate of 10°/min from 25 to 300 °C in air. The oxide content in the membranes casted with the precursor was determined by annealing the sample at 800 °C, followed by the oxide residue weighing.

The membrane conductivity was studied using the Z500 PRO impedancemeter (Elins, Russia) in the frequency range of 10–2·10⁶ Hz in the potentiostatic mode with a sinusoidal excitation voltage of 80 mV with graphite electrodes. The temperature dependence of the conductivity

was investigated in a range from 25 °C to 160 °C with a step of 10–15 °C. The conductivity measurements at different relative humidities (RH) and constant temperature of 90 °C were carried out in the Binder MKF115 climatic chamber. Prior to the measurements, the membranes were kept at each RH for 1 h. The ionic conductivity was calculated by extrapolation of the semicircle corresponding to the bulk conductivity to the real axis.

The gas permeability of the samples was studied using the Crystallux-4000 M gas chromatograph, according to the procedure reported previously [39].

Results and discussion

According to the SEM data, the SiO₂Im-ex sample consists of spherical agglomerates (about 200–700 nm in diameter). The IR-spectrum of the obtained oxide, along with the Si-O bands, shows a band at 1650 cm^{−1} attributed to the C=N bond vibrations. According to the CHN-analysis, the atomic carbon/nitrogen ratio in the obtained silica is 2.7, which is close to the calculated value (3.0). These data confirm the presence of the grafted propyl-imidazoline group on the SiO₂Im-ex oxide surface.

According to the X-ray diffraction analysis, all the composite membranes are amorphous, and the silica incorporation does not change their crystallinity.

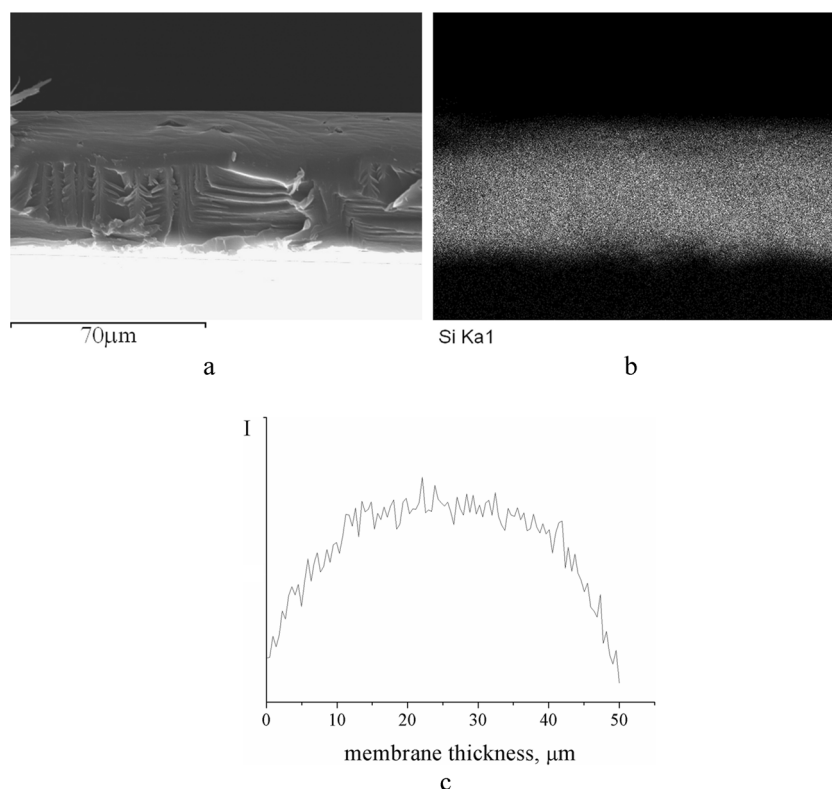
Influence of the precursor hydrolysis conditions on the membrane properties

The influence of the hydrolysis conditions (temperature, medium acidity, treatment time) on the size of silica particles and proton conductivity of the obtained composite membranes was investigated. For this purpose, the hybrid membranes were casted from the mixture of PBI-O-PhT and TEOS solutions with a designed silica loadings (5 and 10 wt%). Hereafter this silica is denoted as SiO₂-in.

Table 1 The silica content in the PBI/SiO₂Im-in membranes according to TGA

Designed silica loading, wt%	Silica content according to TGA, wt%		
	PBI-O-PhT	PBI-2,5Py	PBI-2,6Py
2	1.0	1.9	1.6
5	3.5	4.2	3.9
10	6.7	7.0	7.1
15	10.0	10.4	9.8
20	13.4	13.8	14.9

Fig. 3 SEM-micrograph of a cross-section of the PBI-O-PhT/SiO₂-in-10 membrane (a), the Si mapping (b) and Si distribution across the membrane cross section (c)



Each sample was divided into several equal parts, which were hydrolyzed with either 12% NH₄OH solution or 18% HCl solution at different temperatures for different time.

As seen in the TEM micrographs in Fig. 2, hydrolysis in the acidic medium yields to the formation of the isolated silica particles of 15–20 nm, whereas in the alkaline medium, their size is reduced to 2–5 nm. At higher temperatures in the alkaline medium, the particle size increases up to 6–8 nm (Fig. 2c). The membranes with larger particles were found to have somewhat lower conductivity. Therefore, in further studies, the hydrolysis of the silanes within the PBI matrix was carried out by the ammonium hydroxide solution at 25°C.

Hybrid membranes with functionalized silica

The real silica content in the membranes obtained by the 2nd method was lower compared with the designed values (Table 1). It can be attributed to a partial precursor leaching during hydrolysis. According to the EDX analysis, the silicon concentration in the membrane surface layer (up to 10 μm) is slightly lower than that in the membrane bulk (Fig. 3). As in the previously reported composite PBI membranes with sulfonated silica [34], after annealing of hybrid membranes, fused nanoparticles with the Si/O molar ratio of 1:2 are formed (EDX microanalysis).

Incorporation of the silica nanoparticles with basic nitrogen atoms on the surface leads to an increase in the doping degree

Table 2 The phosphoric acid doping degree for the PBI hybrid membranes

Designed silica loading, wt%	The phosphoric acid doping degree for the PBI-					
	-O-PhT SiO ₂ Im-ex	-2,5Py	-2,6Py	-O-PhT SiO ₂ Im-in	-2,5Py	-2,6Py
0	9.3	6.4	5.2	9.3	6.4	5.2
2	9.4	6.5	5.3	9.7	6.4	5.3
5	9.5	6.5	5.4	9.9	6.6	5.4
10	9.8	6.7	5.5	10.2	7.0	5.6
15	10.2	6.8	5.7	10.6	7.2	5.8
20	10.5	7.0	5.8	10.7	7.7	6.0

Table 3 The water uptake of the PBI hybrid membranes doped with phosphoric acid

Designed silica loading, wt%	Water uptake (%) for the PBI-					
	-O-PhT SiO ₂ Im-ex	-2,5Py	-2,6Py	-O-PhT SiO ₂ Im-in	-2,5Py	-2,6Py
0	9.7	17.0	14.9	9.7	17.0	14.9
2	10.1	17.1	15.6	9.7	17.2	15.0
5	10.3	17.0	15.9	9.8	17.7	15.1
10	10.2	17.1	15.7	9.9	18.0	15.2
15	10.2	16.5	15.7	10.0	18.2	15.3
20	9.9	16.0	15.4	10.1	18.4	15.6

of phosphoric acid for all the studied polymers (Table 2). The most pronounced increase is observed in the case of membrane modification with SiO₂Im-in (the 2nd method). It is probably due to its smaller particle size compared with that of SiO₂Im-ex or a higher sorption ability. The interactions between 3-(2-imidazolin-1-yl)propyl group of silica and nitrogen atoms of PBI can also play a role in packing of PBI chains and lead to an increase in the distance between them [40]. As a result, the grafted functional groups of silica and the nitrogen atoms of the PBI itself become more accessible to the acid. Probably, the same factors provide the discrepancy in the phosphoric acid doping degree between the PBI-2,5Py and PBI-2,6Py membranes, the composition of which is identical, and the only difference is the relative position of imidazole fragment and the nitrogen atom of the pyridine ring to each other in the monomer.

The presence of the silica precursor during membrane formation results in increase in both the phosphoric acid doping degree and the water uptake. Thus, the modification with SiO₂Im-in results in increased water uptake for all the studied membranes (Table 3). In the case of the SiO₂Im-ex incorporation, the water uptake of the PBI-O-PhT and PBI-2,6Py membranes is almost independent on the silica content.

Whereas for the PBI-2,5Py membranes, the water uptake even decreases at high silica loadings (Table 3). Incorporation of the pre-synthesized silica particles is apparently less efficient due to their large size. This leads to a contraction of the polymer free volume which can be occupied by water. The increase in the phosphoric acid doping degree in this case is mostly due to the interaction of H₃PO₄ with the grafted basic groups of silica.

With relative humidity increase, the conductivity growth is observed for all the PBI-based hybrid membranes (Fig. 4). This effect is most pronounced in the case of PBI-Py membranes. For the membranes obtained by the 1st method, the highest conductivity increase is 26% for the PBI-O-PhT/SiO₂Im-ex-15 membrane (at RH = 50%) and 43% for the PBI-2,6Py/SiO₂Im-ex-10 membrane (at RH = 85%). For the membranes obtained by the 2nd method, the conductivity increases up to 32% for the PBI-2,6Py/SiO₂Im-in-10 membrane (at RH = 50%) and 40% for the PBI-O-PhT/SiO₂Im-in-10 (at RH = 50%). The reason for the conductivity enhancement is the increase in charge carrier concentration due to a larger dissociation degree of phosphoric acid in a more dilute solution within the pores. In addition, the increase in relative humidity leads to decrease of the viscosity of the “solution”

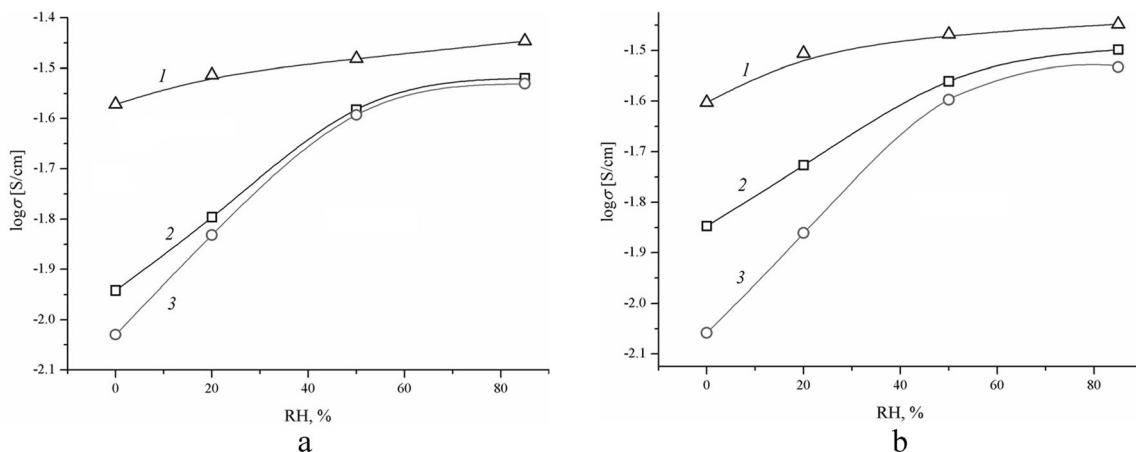


Fig. 4 Plots of conductivity versus relative humidity at 90°C for the PBI-O-PhT (1), PBI-2,5Py (2), PBI-2,6Py (3) membranes containing 15 wt% of SiO₂Im-ex (a) and 15 wt% of SiO₂Im-in (b)

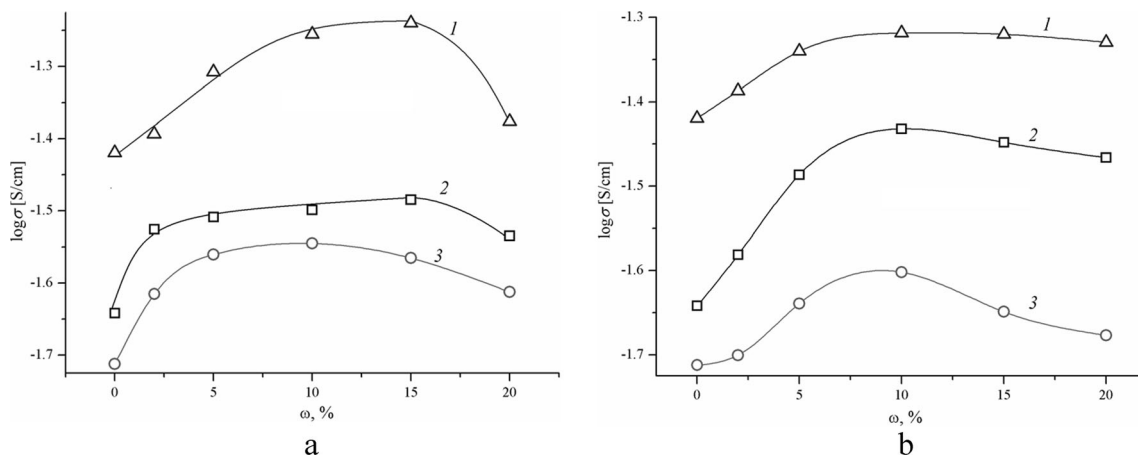


Fig. 5 Plots of conductivity versus composition at 120°C for the PBI-O-PhT (1), PBI-2,5Py (2), PBI-2,6Py (3) hybrid membranes containing $\text{SiO}_2\text{Im-ex}$ (a) and $\text{SiO}_2\text{Im-in}$ (b)

within the membrane (due to an increased water uptake), thus promoting an increase in ion mobility and consequently in conductivity.

The temperature dependence of the conductivity in composite membranes without additional wetting shows a conductivity enhancement with the modified silica incorporation regardless of the membrane preparation method (Fig. 5). For the hybrid membranes obtained by the 1st method, the maximum in the conductivity-composition curves appears to be at 5–15 wt% of $\text{SiO}_2\text{Im-ex}$ (Fig. 5a). Further increase in its content leads to a decrease in the hybrid membrane conductivity. For the membranes modified by the 2nd method, the highest conductivity increase is observed for the PBI-2,5Py-based samples (Fig. 5b). The difference in the structure of the obtained hybrid membranes (relative position and packing of polymer chains) has a significant impact on the observed composition effect.

The conductivity of the polybenzimidazole-based membranes is due to the absorbed phosphoric acid. The most likely mechanism of proton transfer in such systems is the Grotthuss mechanism, which assumes that the imidazole groups of PBI membrane, phosphoric acid, and its dissociation products are all involved in the proton transport [41]. The incorporation of the surface-functionalized silica leads to a binding of additional H_3PO_4 by the grafted imidazole groups and to the expansion of the inner polymer volume. Moreover, silica particles and nitrogen atoms of the grafted functional groups can serve as additional proton transfer centers, which should increase the transfer rate.

In [42, 43], the PBI membranes with different SiO_2 -based fillers were investigated. Similarly, it was shown an increase in the conductivity at low silica content (5 wt%) and conductivity decrease for higher filler contents. The authors attribute this to the formation of more favorable pathways for the proton transport around the silica particles at low filler content, whereas at a higher silica loading, there is a physical barrier for the H^+ transfer due to the intrinsic resistivity of the filler phase [42].

Such a result is similar to that in the composite proton-exchange perfluorinated membranes used in low-temperature fuel cells. The conductivity increase for them is usually observed at low filler content. In the framework of the model of limited elasticity of the membrane pore walls, this is due to the expansion of the channels connecting the pores and an increase in the pore volume [44]. With the further increase in the content and the size of filler particles, the pore can no longer be deformed and additional barriers for ion transfer appear in the membrane [44]. This analogy is not strict, since there are no pores and channels in the pristine PBI membranes. However, they appear after doping with phosphoric acid, which is introduced between the polymer chains. Moreover, another model of the perfluorinated membranes structure in which the pore system is replaced by the comb-shaped channels [45, 46] makes this analogy more reasonable.

The gas permeability plays an important role in the membrane operation in fuel cells. Incorporation of small amounts of

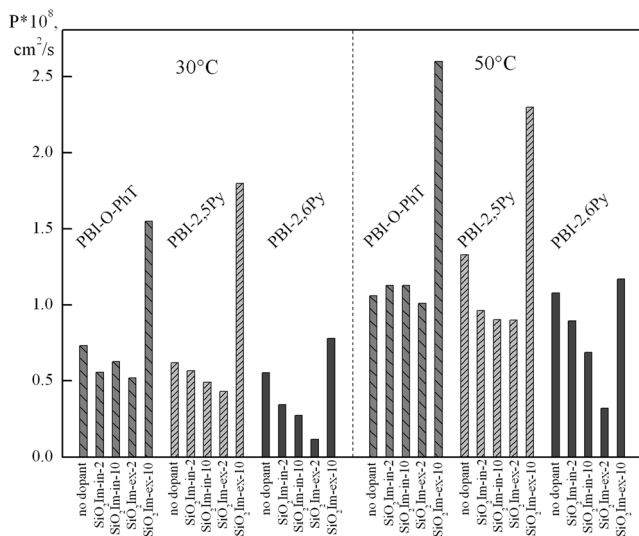


Fig. 6 Hydrogen permeability (cm^2/s) at 30 and 50°C for the PBI-based composite membranes doped with H_3PO_4

surface-modified silica results in a decrease of hydrogen permeability (Fig. 6). In most cases, a higher decrease was found for the SiO₂Im-ex-based membranes. The increase in the SiO₂Im-ex concentration leads to a considerable enhancement of gas permeability, whereas in the case of SiO₂Im-in, an opposite effect is observed. According to the classic Maxwell model, the gas permeability should decrease upon incorporation of impermeable particles. However, this effect is usually observed at a high filler content [47]. In contrast, nanoparticles can prevent the tight packing of rigid polymer chains and thus promote the formation of pores which increase gas permeability. The less is the particle size, the smaller the effect can be. For the composite membranes filled with 2 wt% of SiO₂-in, the described effect is larger, which is confirmed by the data on the phosphoric acid doping degree and water uptake. As a result, the gas permeability is higher compared to the PBI/SiO₂-ex-2 membrane. On the contrary, incorporation of small particles often prevents gas permeation through ion-exchange polymers with solution-filled pores. In particular, this effect is typical for the membranes used in fuel cells [8].

Conclusion

In summary, the membrane modification by silica with grafted basic groups increases the conductivity at low dopant content regardless of the hybrid membranes preparation method. The in situ method makes it possible to obtain membranes with nanoparticles uniformly distributed over the membrane. The higher composite effect is observed for the PBI-2,5Py membranes obtained by casting the polymer with the precursor. Incorporation of small amounts of the dopant promotes the reduction of gas permeability of the membranes. The method of silica incorporation has a significant impact on transport properties of the obtained materials.

Acknowledgments The authors thank Dr. Nataliya Tabachkova for TEM measurements. The scanning electron microscopy and CHN-analysis were performed using shared experimental facilities supported by IGIC RAS state assignment.

Funding information The work was financially supported by the Russian Science Foundation (project N 17-73-10447).

References

- Girard JE (2014) Principles of environmental chemistry, 3rd edn. USA, Jones & Bartlett Learning
- Popel' OS, Tarasenko AB (2011) Modern kinds of electric energy storages and their application in independent and centralized power systems. *Therm Eng* 58:883–893. <https://doi.org/10.1134/S0040601511110103>
- Ellabban O, Abu-Rub H, Blaabjerg F (2014) Renewable energy resources: current status, future prospects and their enabling technology. *Renew Sust Energ Rev* 39:748–764. <https://doi.org/10.1016/j.rser.2014.07.113>
- Hu H, Xie N, Fang D, Zhang X (2018) The role of renewable energy consumption and commercial services trade in carbon dioxide reduction: evidence from 25 developing countries. *Appl Energy* 211:1229–1244. <https://doi.org/10.1016/j.apenergy.2017.12.019>
- O'Connell N, Pinson P, Madsen H, O'Malley M Benefits and challenges of electrical demand response: A critical review. *Renew Sust Energ Rev* 39(2014):686–699. <https://doi.org/10.1016/j.rser.2014.07.098>
- Cebulla F, Naegler T, Pohl M (2017) Electrical energy storage in highly renewable European energy systems: capacity requirements, spatial distribution, and storage dispatch. *J Energy Storage* 14:211–223. <https://doi.org/10.1016/j.est.2017.10.004>
- Paterakis NG, Erdinç O, Catalão JPS (2017) An overview of demand response: key-elements and international experience. *Renew Sust Energ Rev* 69:871–891. <https://doi.org/10.1016/j.rser.2016.11.167>
- Stenina IA, Yaroslavtsev AB (2017) Nanomaterials for lithium-ion batteries and hydrogen energy. *Pure Appl Chem* 89:1185–1194. <https://doi.org/10.1515/pac-2016-1204>
- Weitemeyer S, Kleinhans D, Vogt T, Agert C (2015) Integration of renewable energy sources in future power systems: the role of storage. *Renew Energy* 75:14–20. <https://doi.org/10.1016/j.renene.2014.09.028>
- Guney MS, Tepe Y (2017) Classification and assessment of energy storage systems. *Renew Sust Energ Rev* 75(C):1187–1197. <https://doi.org/10.1016/j.rser.2016.11.102>
- Tsodikov MV, Kurdyumov SS, Konstantinov GI, Murzin VY, Bukhtenko OV, Maksimov YV (2015) Core-shell bifunctional catalyst for steam methane reforming resistant to H₂S: activity and structure evolution. *Int J Hydrog Energy* 40:2963–2970. <https://doi.org/10.1016/j.ijhydene.2015.01.016>
- Basov NL, Ermilova MM, Orekhova NV, Yaroslavtsev AB (2013) Membrane catalysis in the dehydrogenation and hydrogen production processes. *Russian Chem Rev* 82:352–368. <https://doi.org/10.1070/RC2013v082n04ABEH004324>
- Sansaniwal SK, Pal K, Rosen MA, Tyagi SK (2017) Recent advances in the development of biomass gasification technology: a comprehensive review. *Renew Sust Energ Rev* 72:363–384. <https://doi.org/10.1016/j.rser.2017.01.038>
- Li Q, Jensen JO, Savinell RF, Bjerrum NJ (2009) High temperature proton exchange membranes based on polybenzimidazoles for fuel cells. *Prog Polym Sci* 34:449–477. <https://doi.org/10.1016/j.procpolymsci.2008.12.003>
- Yaroslavtsev AB, Stenina IA, Kulova TL, Skundin AM, Desyatov AV (2019) Nanomaterials for Electrical Energy Storage, in: D.L. Andrews, T. Nann, R.H. Lipson (Eds.), *Comprehensive nanoscience and nanotechnology*, Second edition, V.5 Application of nanoscience, Amsterdam, Boston, Heidelberg, London, New York, Oxford, Paris, San Diego, San Francisco, Singapore, Sydney, Tokio: Elsevier. Academic. Press, pp. 165–206
- An L, Zeng L, Zhao TS (2013) An alkaline direct ethylene glycol fuel cell with an alkali-doped polybenzimidazole membrane. *Int J Hydrog Energy* 38:10602–10606. <https://doi.org/10.1016/j.ijhydene.2013.06.042z>
- Wu QX, Pan ZF, An L (2018) Recent advances in alkali-doped polybenzimidazole membranes for fuel cell applications. *Renew Sust Energ Rev* 89:168–183. <https://doi.org/10.1016/j.rser.2018.03.024>
- Giffin GA, Galbiati S, Walter M, Aniol K, Ellwein C, Kerres J, Zeis R (2017) Interplay between structure and properties in acid-base blend PBI-based membranes for HT-PEM fuel cells. *J Membr Sci* 535:122–131. <https://doi.org/10.1016/j.memsci.2017.04.019>
- Özdemir Y, Özkan N, Devrim Y (2017) Fabrication and characterization of cross-linked polybenzimidazole based membranes for

- high temperature PEM fuel cells. *Electrochim Acta* 245:1–13. <https://doi.org/10.1016/j.electacta.2017.05.111>
20. Sun X, Simonsen SC, Norby T, Chatzidakis A (2019) Composite membranes for high temperature PEM fuel cells and electrolyzers: a critical review. *Membr*. 9:83. <https://doi.org/10.3390/membranes9070083>
 21. Wang L, Liu Z, Liu Y, Wang L (2019) Crosslinked polybenzimidazole containing branching structure with no sacrifice of effective N-H sites: towards high-performance high-temperature proton exchange membranes for fuel cells. *J Membr Sci* 583: 110–117. <https://doi.org/10.1016/j.memsci.2019.04.030>
 22. Haque MA, Sulong AB, Loh KS, Majlan EH, Husaini T, Rosli RE (2017) Acid doped polybenzimidazoles based membrane electrode assembly for high temperature proton exchange membrane fuel cell: a review. *Int J Hydr Energy* 42:9156–9179. <https://doi.org/10.1016/j.ijhydene.2016.03.086>
 23. Araya SS, Zhou F, Liso V, Sahlin SL, Vang JR, Thomas S, Gao X, Jeppesen C, Kær SK (2016) A comprehensive review of PBI-based high temperature PEM fuel cells. *Int J Hydr Energy* 41:21310–21344. <https://doi.org/10.1016/j.ijhydene.2016.09.024>
 24. Schmidt TJ, Baummeister J (2008) Properties of high-temperature PEFC Celtec®-P 1000 MEAs in start/stop operation mode. *J Power Sources* 176:428–434. <https://doi.org/10.1016/j.jpowsour.2007.08.055>
 25. Stenina IA, Yaroslavtsev AB (2017) Low- and intermediate-temperature proton-conducting electrolytes. *Inorg Mater* 53:253–262. <https://doi.org/10.1134/S0020168517030104>
 26. Arlt T, Maier W, Tötze C, Wanek C, Markötter H, Wieder F, Banhart J, Lehnert W, Manke I (2014) Synchrotron X-ray radioscopic in situ study of high-temperature polymer electrolyte fuel cells - effect of operation conditions on structure of membrane. *J Power Sources* 246:290–298. <https://doi.org/10.1016/j.jpowsour.2013.07.094>
 27. Zhang J, Aili D, Bradley J, Kuang H, Pan C, De Marco R, Li Q, Jiang SP (2017) In situ formed phosphoric acid/phosphosilicate nanoclusters in the exceptional enhancement of durability of polybenzimidazole membrane fuel cells at elevated high temperatures. *J Electrochem Soc* 164(14):F1615–F1625. <https://doi.org/10.1149/2.1051714jes>
 28. Lysova AA, Ponomarev II, Yaroslavtsev AB (2011) Composite materials based on polybenzimidazole and inorganic oxides. *Solid State Ionics* 188:132–134. <https://doi.org/10.1016/j.ssi.2010.10.010>
 29. Özdemir Y, Üregen N, Devrim Y (2017) Polybenzimidazole based nanocomposite membranes with enhanced proton conductivity for high temperature PEM fuel cells. *Int J Hydr Energy* 42:2648–2657. <https://doi.org/10.1016/j.ijhydene.2016.04.132>
 30. Sun P, Li Z, Wang S, Yin X (2018) Performance enhancement of polybenzimidazole based high temperature proton exchange membranes with multifunctional cross-linker and highly sulfonated polyaniline. *J Membr Sci* 549:660–669. <https://doi.org/10.1016/j.memsci.2017.10.053>
 31. Wang S, Sun P, Li Z, Liu G, Yin X (2018) Comprehensive performance enhancement of polybenzimidazole based high temperature proton exchange membranes by doping with a novel intercalated proton conductor. *Int J Hydr Energy* 43:9994–10003. <https://doi.org/10.1016/j.ijhydene.2018.04.089>
 32. Cheng Y, Zhang J, Lu S, Kuang H, Bradley J, De Marco R, Aili D, Li Q, Cui CQ, Jiang SP (2018) High CO tolerance of new SiO₂ doped phosphoric acid/polybenzimidazole polymer electrolyte membrane fuel cells at high temperatures of 200–250°C. *Int J Hydr Energy* 43:22487–22499. <https://doi.org/10.1016/j.ijhydene.2018.10.036>
 33. Lysova AA, Stenina IA, Volkov AO, Ponomarev II, Yaroslavtsev AB (2019) Proton conductivity of hybrid membranes based on polybenzimidazoles and surface-sulfonated silica. *Solid State Ionics* 329:25–30. <https://doi.org/10.1016/j.ssi.2018.11.012>
 34. Lysova AA, Stenina IA, Volkova YA, Ponomarev II, Yaroslavtsev AB (2019) Effect of surface-sulfonated silica on the properties of pyridine-containing polybenzimidazoles. *Membr and Membr Technol* 1:271–277
 35. Mikheev AG, Safronova EY, Yurkov GY, Yaroslavtsev AB (2013) Hybrid materials based on MF-4SC perfluorinated sulfo cation-exchange membranes and silica with proton-acceptor properties. *Mendeleev Commun.* 23:66–68. <https://doi.org/10.1016/j.mencom.2013.03.002>
 36. Quartarone E, Angioni S, Mustarelli P (2017) Polymer and composite membranes for proton-conducting, high-temperature fuel cells: a critical review. *Mater* 10:687. <https://doi.org/10.3390/ma10070687>
 37. Kumar S, Sana B, Mathew D, Unnikrishnan G, Jana T, Kumar KSS (2018) Polybenzimidazole-nanocomposite membranes: enhanced proton conductivity with low content of amine-functionalized nanoparticles. *Polymer* 145:434–446. <https://doi.org/10.1016/j.polymer.2018.04.081>
 38. Fomenkov AI, Blagodatskikh IV, Ponomarev II, Volkova YA, Ponomarev II, Khokhlov AR (2009) Synthesis and molecular-mass characteristics of some cardo poly(benzimidazoles). *Polym Sci Ser B* 51:166–173. <https://doi.org/10.1134/S1560090409050030>
 39. Lysova AA, Ponomarev II, Volkova YA, Ponomarev II, Yaroslavtsev AB (2018) Effect of phosphorylation of polybenzimidazole on its conductive properties. *Petroleum Chem* 58:958–964. <https://doi.org/10.1134/S0965544118110038>
 40. Sadeghi M, Semsarzadeh MA, Moadel H (2009) Enhancement of the gas separation properties of polybenzimidazole (PBI) membrane by incorporation of silica nano particles. *J Membr Sci* 331: 21–30. <https://doi.org/10.1016/j.memsci.2008.12.073>
 41. Melchior J-P, Majer G, Kreuer K-D (2017) Why do proton conducting polybenzimidazole phosphoric acid membranes perform well in high-temperature PEM fuel cells? *Phys Chem Chem Phys* 19:601–612. <https://doi.org/10.1039/C6CP05331A>
 42. Quartarone E, Magistris A, Mustarelli P, Grandi S, Carollo A, Zukowska GZ, Garbarczyk JE, Nowinski JL, Gerbaldi C, Bodoardo S (2009) Pyridine-based PBI composite membranes for PEMFCs. *Fuel Cells* 9:349–355. <https://doi.org/10.1002/fuce.200800149>
 43. Quartarone E, Mustarelli P, Carollo A, Grandi S, Magistris A, Gerbaldi C (2009) PBI composite and nanocomposite membranes for PEMFCs: the role of the filler. *Fuel Cells* 9:231–236. <https://doi.org/10.1002/fuce.200800145>
 44. Novikova SA, Safronova EY, Lysova AA, Yaroslavtsev AB (2010) Influence of incorporated nanoparticles on the ionic conductivity of MF-4SC membrane. *Mendeleev Commun* 20:156–157. <https://doi.org/10.1016/j.mencom.2010.05.011>
 45. Rebrov AV, Ozerin AN, Svergun DI, Bobrova LP, Bakeev NF (1990) Study of aggregation of macromolecules of perfluorosulfonated ionomer in solution by the small-angle X-ray-scattering method. *Polym Sci USSR* 32:1515–1521. [https://doi.org/10.1016/0032-3950\(90\)90068-H](https://doi.org/10.1016/0032-3950(90)90068-H)
 46. Yaroslavtsev AB (2013) Perfluorinated ion-exchange membranes. *Polym Sci Ser A* 55:674–698. <https://doi.org/10.1134/S0965545X13110060>
 47. Yaroslavtsev AB, Yampolskii YP (2014) Hybrid membranes containing inorganic nanoparticles. *Mendeleev Commun.* 24:319–326. <https://doi.org/10.1016/j.mencom.2014.11.001>

Publisher's note Springer Nature remains neutral with regard to jurisdictional claims in published maps and institutional affiliations.